

Entanglement Characteristics of a Spin-Boson Quantum Phase Transition.

N. Lambert,¹ C. Emery,² and T. Brandes¹

¹*The University of Manchester, P.O. Box 88, Manchester, M60 1QD, U.K.*

²*Instituut-Lorentz, Universiteit Leiden, P.O. Box 9506, 2300 RA Leiden, The Netherlands*

(Dated: May 23, 2019)

We investigate the entanglement properties of an ensemble of atoms interacting with a single bosonic field mode via the Dicke (superradiance) Hamiltonian. The model exhibits a quantum phase transition and a well-understood thermodynamic limit, allowing the identification of both quantum and semi-classical many-body features in the behavior of the entanglement. We consider entanglement between the atoms and field, as well both bi- and multi-partite entanglement between atoms. In the thermodynamic limit, we give exact results for all entanglement partitions and observe a logarithmic divergence of the atom-field entanglement, and discontinuities in the pairwise and multipartite entanglement.

I. INTRODUCTION

Understanding entanglement – the quantum correlations impossible to mimic with local classical theories – is a fundamental goal of quantum information science. Similarly, understanding complex modes of behavior, such as quantum phase transitions [1] and quantum chaos [2], has become an important part of quantum many-body theory. Since large correlations and collective behavior are an intrinsic part of critical systems, concepts and formalisms used to describe entanglement are now being employed to reveal the truly quantum nature of certain aspects of criticality.

Investigations into the entanglement between interacting spin-1/2 systems on a one dimensional chain have revealed so-called ‘critical entanglement’, in which an entanglement measure of the ground state exhibits universality, or scaling behavior, around the critical point [3]. In particular, for the infinite XY spin chains, (and their Ising variants) it has been shown that entanglement between nearest and next-nearest neighbors reaches a maximum *near*, but not at, the critical point [3, 4]. Furthermore, Osterloh *et al.* [4] have observed scaling behavior of the entanglement, showing that the derivative of the concurrence diverges logarithmically near the critical point. They also found a logarithmic divergence of the derivative as a function of system size.

Latorre, Vidal, and co-workers [5, 6] took a different approach and investigated the entanglement, via the von Neumann entropy, between a block of L spins and the rest of the chain in XY and Heisenberg spin-chains. They found a logarithmic scaling of the entropy with L ; this time with a pre-factor corresponding to the ‘central charge’ of a 1+1 continuum quantum field theory of the same universality class. In effect, they found the same area law associated with the geometric entropy first studied by Srednicki [7]. In an effort to understand the nature of the scaling of entanglement, Orús *et al.* [8] illustrate that the scaling of the entanglement at the critical point determines whether or not one could efficiently simulate the quantum system at this point on a classical computer.

Going beyond 1-dimensional spin chains, the authors

of [9] studied a highly connected simplex, where each spin interacts equally with all other spins, and the lattice spacing no longer plays an important role. Importantly, because of the symmetry, they find a maximum in the pairwise concurrence at the critical point, and determine scaling exponents for the behaviour of the concurrence with system size.

In this paper, we calculate the entanglement properties of the single-mode Dicke Hamiltonian, which describes an ensemble of N two-level atoms coupled to a single-mode bosonic field. This model exhibits a ‘superradiant’ quantum phase transition (QPT) in which the ground state undergoes a dramatic change in character. We consider several aspects of the ground-state entanglement in this model and observe how they are affected by the QPT. We investigate entanglement between the atomic ensemble and the field mode via the von Neumann entropy [10, 11] of this bipartite decomposition. We also calculate the entanglement between pairs of the atoms in the ensemble via the concurrence [12, 13], and obtain insight into the multipartite entanglement in the ensemble by considering a simple measure of global entanglement based on the work of Meyer and Wallach [14]. In the thermodynamic limit, the model is exactly soluble across the whole coupling range, and we give exact results for these three quantifiers of the entanglement in this limit. For finite N we use perturbative and numerical methods.

The atom-field entropy is observed to diverge at the phase transition alongside the traditional correlation length, with corresponding critical exponents, and may be fruitfully described by an effective ‘entanglement temperature’. The re-scaled pairwise concurrence and the multipartite measure Q both have divergences in their derivatives at the critical point.

As has been discussed previously [15, 16], the QPT is foreshadowed at finite N by various ‘precursors’, and in particular, a transition from integrable to Quantum Chaotic behavior near the critical point. This transition is characterized by a change in energy level statistics, and can be correlated with the change in the phase-space of a classical Hamiltonian corresponding to Dicke model. The phase transition in the quantum model maps to a super-

critical pitchfork bifurcation in the classical model, and such bifurcations have recently been related to entanglement characteristics [17, 18]. In addition, Fujisaki *et al.* have shown that the appearance and strength of chaos can be linked to the production of entanglement [19]. Further work is required in clarifying the relation between entanglement in quantum systems and chaos in the corresponding classical model. However, there is a conceptual connection between the divergence of trajectories in classical chaos and the delocalization of the quantum ground state, which is, in general, indicative of entanglement.

The model considered here is of wider interest still, given that the interaction of a charge or spin systems with a single bosonic mode is viewed as a mechanism for generation of entanglement in many different situations such as quantum cavity QED, quantum dots [20, 21], and ion traps. In addition, many suggestions have been made to use the environment, or bosonic cavities, to share or mediate entanglement [20, 22, 23, 24].

The paper has the following structure. In section II we introduce the Dicke Hamiltonian, and describe the quantum phase transition. In section III we consider the atom-field entanglement. We first look at numerical results for finite N , and then describe the exact results in the thermodynamic limit. We follow this with a comparison of the von Neumann entropy, the linear entropy, and inverse participation ratio. In section IV we calculate the concurrence between two atoms in the ensemble. The multipartite entanglement is considered in section V both at finite N and in the thermodynamic limit. We conclude with discussions in section VI.

II. THE DICKE MODEL

Generically, the Dicke Hamiltonian (DH) describes the dipole interaction between N atoms and n bosonic field modes. Here we shall only consider the single mode case with $n = 1$. A standard approach to such quantum-optics Hamiltonians is to make the rotating wave approximation (RWA), rendering the model integrable. We do not make the RWA here, allowing the model to describe both weak and strong coupling regimes.

A. The Hamiltonian

The single-mode Dicke Hamiltonian is

$$\begin{aligned} H &= \omega_0 \sum_{i=1}^N s_z^{(i)} + \omega a^\dagger a + \sum_{i=1}^N \frac{\lambda}{\sqrt{N}} (a^\dagger + a) (s_+^{(i)} + s_-^{(i)}) \\ &= \omega_0 J_z + \omega a^\dagger a + \frac{\lambda}{\sqrt{2j}} (a^\dagger + a) (J_+ + J_-), \end{aligned} \quad (1)$$

where $J_z = \sum_{i=1}^N s_z^i$, $J_\pm = \sum_{i=1}^N s_\pm^i$ are collective angular momentum operators for a pseudo-spin of length $j = N/2$. These operators obey the usual angular momentum commutation relations, $[J_z, J_\pm] = \pm J_\pm$ and

$[J_+, J_-] = 2J_z$. The frequency ω_0 describes the atomic level splitting, ω is the field frequency, and λ the atom-field coupling strength.

There exists a conserved parity operator

$$\Pi = e^{i\pi(a^\dagger a + J_z + j)}, \quad (2)$$

which commutes with the Hamiltonian. For finite N , the ground state has positive parity. The DH undergoes a QPT at a critical value of the atom-field coupling $\lambda_c = \sqrt{\omega\omega_0}/2$ which breaks this symmetry.

We make use of the parity symmetry to simplify numerical calculations. At finite N , we perform numerical diagonalisations using a basis $|n\rangle \otimes |j, m\rangle$, where $|n\rangle$ are Fock states of the field, and $|j, m\rangle$ are the so-called Dicke states – eigenstates of \mathbf{J}^2 and J_z .

B. Thermodynamic Limit

The DH undergoes a QPT in the thermodynamic limit ($j \rightarrow \infty \Leftrightarrow N \rightarrow \infty$, notation which we will use interchangeably) at a critical coupling of $\lambda_c = \sqrt{\omega\omega_0}/2$. Below λ_c the system is in its normal phase in which the ground state is largely unexcited. Above λ_c , the superradiant phase, the ground-state possesses a macroscopic excitation.

As illustrated in Ref. [15], exact solutions may be obtained for both phases in the thermodynamic limit by employing a Holstein-Primakoff transformation of the angular momentum algebra. In this section, we briefly summarize this analysis, highlighting those features such as are required here.

The Holstein-Primakoff mapping expresses the angular momentum in terms of a single boson mode,

$$J_+ = b^\dagger \sqrt{2j - b^\dagger b}, \quad J_- = \sqrt{2j - b^\dagger b} b, \quad J_z = b^\dagger b - j, \quad (3)$$

with $[b, b^\dagger] = 1$. In this representation, the DH transforms into a two bosonic mode problem

$$\begin{aligned} H &= \omega_0(b^\dagger b - j) + \omega a^\dagger a \\ &+ \lambda(a + a^\dagger)[b^\dagger \sqrt{(1 - b^\dagger b/2j)} + \sqrt{(1 - b^\dagger b/2j)} b]. \end{aligned} \quad (4)$$

In this representation, the parity operator is $\Pi = e^{i\pi[a^\dagger a + b^\dagger b]}$. We treat the two phases separately in obtaining exact solutions.

1. Normal Phase

By simply taking $j \rightarrow \infty$ in Eq. (5), the square-roots approximate to unity and we obtain

$$H = \omega a^\dagger a + \omega_0 b^\dagger b + \lambda(a + a^\dagger)(b + b^\dagger) - j\omega_0. \quad (5)$$

To diagonalise this Hamiltonian we introduce position and momentum operators for the two bosonic modes.

$$\begin{aligned} x &= \frac{1}{\sqrt{2\omega}}(a + a^\dagger), \quad p_x = i\sqrt{\frac{\omega}{2}}(a^\dagger - a) \\ y &= \frac{1}{\sqrt{2\omega_0}}(b + b^\dagger), \quad P_y = i\sqrt{\frac{\omega_0}{2}}(b^\dagger - b) \end{aligned} \quad (6)$$

Rotating the coordinates $q_1 = -y \sin \gamma^{(1)} + x \cos \gamma^{(1)}$, $q_2 = y \cos \gamma^{(1)} + x \sin \gamma^{(1)}$ by an angle given by

$$\tan(2\gamma^{(1)}) = \frac{4\lambda\sqrt{\omega\omega_0}}{(\omega_0^2 - \omega^2)}, \quad (7)$$

diagonalizes Hamiltonian (5). The resulting normal phase effective Hamiltonian has the two excitation energies

$$\epsilon_{\pm}^{(1)} = \frac{1}{2} \left(\omega^2 + \omega_0^2 \pm \sqrt{(\omega_0^2 - \omega^2)^2 + 16\lambda^2\omega\omega_0} \right). \quad (8)$$

ϵ_- is only real for $\lambda \leq \lambda_c$, giving the range of this solution. Hamiltonian (5) commutes with the parity operator, and thus the ground state of this phase has definite, positive parity.

To calculate the atom-field entanglement of the ground state, we require the reduced density matrix (RDM) of the atoms in the ground state. The position representation introduced in Eqs (6) is very convenient for this calculation.

In terms of the collective coordinates q_1 and q_2 , the ground-state wave function is a product of two Gaussians, $\Psi(q_1, q_2) = G_+(q_1)G_-(q_2)$. Inverting the above coordinate rotations gives us the wave function in terms of the coordinates (x, y) corresponding to the physical field (x) and atom (y) modes. In this representation the ground state density matrix is therefore (writing $c = \cos \gamma^{(1)}$, and $s = \sin \gamma^{(1)}$),

$$\begin{aligned} \rho_G(x, x', y, y') &= \Psi_G^*(x, y)\Psi_G(x', y') \\ &= \left(\frac{\epsilon_+^{(1)}\epsilon_-^{(1)}}{\pi^2} \right)^{\frac{1}{2}} \times \exp \left[-\frac{(\epsilon_-^{(1)}c^2 + \epsilon_+^{(1)}s^2)}{2}(x^2 + x'^2) \right] \\ &\quad \times \exp \left[-\frac{(\epsilon_-^{(1)}s^2 + \epsilon_+^{(1)}c^2)}{2}(y^2 + y'^2) \right] \\ &\quad \times \exp \left[(-\epsilon_+^{(1)} + \epsilon_-^{(1)})cs(xy + x'y') \right]. \end{aligned} \quad (9)$$

To obtain the RDM of the atomic system, we integrate over the x coordinate. We write the resulting RDM in terms of a rescaled y coordinate $y \rightarrow y/\kappa$,

$$\begin{aligned} \rho_G(y, y') &= \left(\frac{\epsilon_+^{(1)}\epsilon_-^{(1)}}{\pi(\epsilon_-c^2 + \epsilon_+s^2)} \right)^{\frac{1}{2}} \\ &\quad \times \exp \left(\frac{2\epsilon_- - \epsilon_+ + D}{4\kappa^2(\epsilon_-c^2 + \epsilon_+s^2)}(y^2 + y'^2) \right) \\ &\quad + \frac{D}{2\kappa^2(\epsilon_-c^2 + \epsilon_+s^2)}yy', \end{aligned} \quad (10)$$

where $D = (\epsilon_- - \epsilon_+)^2c^2s^2$. As this rescaling is effected by a unitary transformation on the atomic system alone, it will not affect the atom-field entanglement. This rescaling does, however, aid in the interpretation of our results, as we shall see later. Note that the RDM for the field mode is the same as above, except with c and s interchanged.

2. Super-Radiant Phase

In the superradiant (SR) phase ($\lambda > \lambda_c$), both atom and field degrees of freedom acquire macroscopic mean-fields. We incorporate these by displacing the two oscillator modes

$$a^\dagger = c^\dagger \pm \sqrt{\alpha}, \quad b^\dagger = d^\dagger \mp \sqrt{\beta}, \quad (11)$$

where α, β are order j . That there are two choices of sign here is significant, as the two choices lead to degenerate solutions – an indication that the parity of the system has been broken in this phase.

By inserting one of the above displacements into the Hamiltonian (5), and setting terms with overall powers of j in the denominator to zero, we obtain an exactly soluble Hamiltonian. Diagonalization requires a specific choice for the displacements $\sqrt{\alpha} = \frac{2\lambda}{\omega}\sqrt{\frac{j}{2}(1-\mu)}$, $\sqrt{\beta} = \sqrt{j(1-\mu)}$, with $\mu = \lambda_c^2/\lambda^2$, and a rotation of the coordinates

$$\begin{aligned} Q_1 &= X \cos \gamma^{(2)} - Y \sin \gamma^{(2)}, \\ Q_2 &= X \sin \gamma^{(2)} + Y \cos \gamma^{(2)}, \end{aligned} \quad (12)$$

with angle of rotation given by

$$\tan(2\gamma^{(2)}) = \frac{2\omega\omega_0\mu^2}{\omega_0^2 - \mu^2\omega^2}. \quad (13)$$

The excitation energies of the SR phase are

$$\epsilon_{\pm}^2 = \frac{1}{2} \left(\frac{\omega_0^2}{\mu^2} + \omega^2 \pm \sqrt{\left(\frac{\omega_0^2}{\mu^2} - \omega^2 \right)^2 + 4\omega^2\omega_0^2} \right). \quad (14)$$

and ϵ_- is real for only for $\lambda \geq \lambda_c$. The effective Hamiltonians derived with either choice of sign in Eq. (11) do not commute with the parity operator Π , and thus we see that this symmetry is broken in the SR phase.

As before, the ground state of the diagonalised Hamiltonian is the product of two Gaussians in Q_1 and Q_2 . To obtain the wave function in terms of the original atomic and field co-ordinates, we must not only perform the rotation $Q_1, Q_2 \rightarrow X, Y$ but also take into account the relationship between the displaced and re-scaled coordinates X, Y and the original atom-field co-ordinates x, y ,

$$X = x \mp \sqrt{\frac{2\alpha}{\omega}}, \quad Y = \sqrt{\frac{\omega_0}{\omega}}y \pm \sqrt{\frac{2\beta}{\omega}}, \quad (15)$$

where $\tilde{\omega} = \frac{\omega_0}{2\mu}(1 + \mu)$. In the displaced (X, Y) frame the wave functions have the same form as in the normal phase, but with different parameters and coefficients. In the original frame (x, y) the wave functions are again the same but displaced from the origin.

The two choices of displacements therefore lead to two wave functions in the x, y representation displaced from the origin in different directions. However, for all finite N , the large- λ ground state is a two-lobed wavefunction, with each lobe corresponding to one of the above solutions. In the thermodynamic limit the superposition of

these two lobes is destroyed, and the ground state becomes single lobed and doubly degenerate [16].

Thus, at finite N , the ground-state wave function has positive parity for all λ , whereas the $N \rightarrow \infty$ results in the SR phase have mixed parity. To obtain a thermodynamic limit ground state with the same parity as the finite- N wave function, we take a superposition of the two degenerate $N \rightarrow \infty$ wave functions with displacements $X = x - \sqrt{2\alpha/\omega}$ and $X = x + \sqrt{2\alpha/\omega}$. Thus we write the positive-parity SR thermodynamic limit ground state as

$$\Psi_G^{\text{SR}}(x, y) = \frac{1}{\sqrt{2}} \left(\sum_{\pm} G_{-}[(x \pm \sqrt{\frac{2\alpha}{\omega}})c - \sqrt{\frac{\omega_0}{\tilde{\omega}}}(y \pm \sqrt{\frac{2\beta}{\omega_0}})s] G_{+}[(x \pm \sqrt{\frac{2\alpha}{\omega}})s + \sqrt{\frac{\omega_0}{\tilde{\omega}}}(y \pm \sqrt{\frac{2\beta}{\omega_0}})c] \right) \quad (16)$$

where G_{\pm} are the normalized Gaussians. Since the two lobes are orthogonal (the displacements are of order \sqrt{N} , and thus the lobes have vanishing overlap), the RDM of the atoms (obtained by tracing over the ‘ x ’ co-ordinate the density matrix corresponding to $\Psi_G^{\text{SR}}(x, y)$) does not contain any off-diagonal cross-terms. Thus, the resulting RDM is a convex combination, or mixture, of the two spatially separated density matrices

$$\begin{aligned} \rho^{\text{SR}}(y, y') = & \frac{1}{2} \rho_G \left[\sqrt{\frac{\omega_0}{\tilde{\omega}}} (y + \sqrt{\frac{2\beta}{\omega_0}}), \sqrt{\frac{\omega_0}{\tilde{\omega}}} (y' + \sqrt{\frac{2\beta}{\omega_0}}) \right] \\ & + \frac{1}{2} \rho_G \left[\sqrt{\frac{\omega_0}{\tilde{\omega}}} (y - \sqrt{\frac{2\beta}{\omega_0}}), \sqrt{\frac{\omega_0}{\tilde{\omega}}} (y' - \sqrt{\frac{2\beta}{\omega_0}}) \right]. \end{aligned} \quad (17)$$

where ρ_G is the same function used for the normal phase.

Having obtained the RDM of the atoms in both phases, we are now in a position to derive the entanglement in the thermodynamic limit. Before we do so, let us just recall the critical exponents of the phase transition [15]. The excitation energy diverges as $\epsilon_- \propto |\lambda_c - \lambda|^{z\nu}$ and the characteristic length diverges as $l_- = \frac{1}{\sqrt{\epsilon_-}} \propto |\lambda - \lambda_c|^{-\nu}$ with the exponents $z = 2$ and $\nu = 1/4$.

III. ATOM-FIELD ENTANGLEMENT

We parameterize the atom-field entanglement by the von Neumann entropy

$$S = -\text{Tr}(\rho \log_2 \rho) \quad (18)$$

with ρ the RDM of the atoms (an identical result is obtained with the field RDM). We present first numerical and perturbative results for finite N , and then our exact solutions in the thermodynamic limit.

We diagonalise the DH in the Fock-Dicke basis, and obtain the RDM of the atoms. This is diagonalised and the von Neumann entropy is obtained from

$$S(\rho) = -\sum_k p_k \log_2 p_k. \quad (19)$$

where p_k are the eigenvalues of the RDM [10]. In Fig.1 we plot the results of these numerical calculations.

From Rayleigh-Schrödinger perturbation theory, we find an N -independent result for the von Neumann entropy for low coupling (with $\sigma = \lambda/(\omega + \omega_0)$)

$$S = -\frac{1}{1 + \sigma^2} \log_2 \left(\frac{1}{1 + \sigma^2} \right) - \frac{\sigma^2}{1 + \sigma^2} \log_2 \left(\frac{\sigma^2}{1 + \sigma^2} \right). \quad (20)$$

This matches the numerical data well for $\lambda/\lambda_c \lesssim 0.4$. Similarly, following Refs. [25, 26] for $\lambda \rightarrow \infty$, we can identify the strong coupling limit ground state as $|\Psi_{GS}\rangle = \frac{1}{\sqrt{2}} \left(|\frac{\sqrt{2j}\lambda}{\omega}, -j_x\rangle + |-\frac{\sqrt{2j}\lambda}{\omega}, j_x\rangle \right)$, where $|\pm \frac{\sqrt{2j}\lambda}{\omega}, \mp j_x\rangle$ is a product of a coherent state for the field and an eigenstate of J_x for the atoms. As this is effectively a maximally entangled state of two two-level systems, $S \rightarrow 1$ as $\lambda \rightarrow \infty$.

A. Thermodynamic limit

We now use the thermodynamic limit RDMs found above to obtain an exact analytical expression for the entropy S as $N \rightarrow \infty$. This calculation proceeds via comparison with the density matrix of a single harmonic

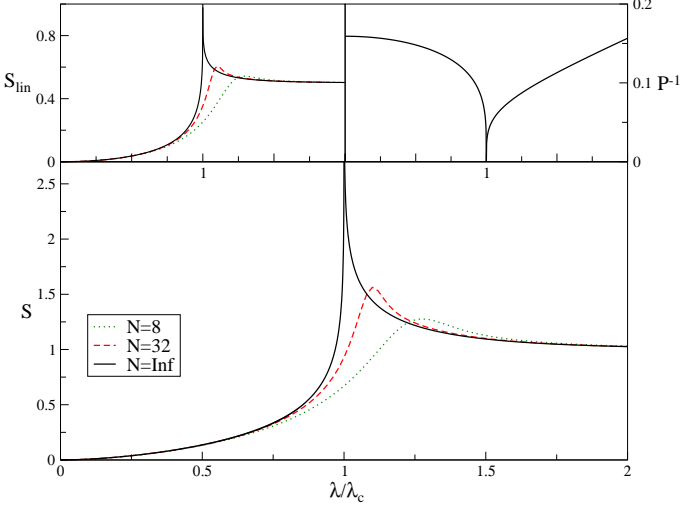


FIG. 1: The von Neumann entropy S between the atomic and bosonic modes for a range of system sizes, $N = 8$, $N = 32$, and $N = \infty$. The divergence at $\lambda/\lambda_c = 1$ can be clearly seen, as well as the strong coupling $S = 1$ limit. The smaller graphs depict the linear entropy S_{lin} between the atomic and bosonic modes, and the inverse participation ratio P^{-1} of the ground state wave-function. The linear entropy exhibits the same behavior as the von Neumann entropy, while the participation ratio drops to 0 at the critical point, indicating a massive delocalization of the ground state.

oscillator of mass m , frequency Ω at temperature T [27]

$$\rho(y, y'; T) = \left(\frac{m\Omega}{4\pi\hbar \sinh(\frac{\hbar\Omega}{k_B T})(\cosh(\frac{\hbar\Omega}{k_B T}) - 1)} \right)^{\frac{1}{2}} \times \exp \left[\frac{-m\Omega}{2\hbar \sinh(\frac{\hbar\Omega}{k_B T})} \left((y^2 + y'^2) \cosh(\frac{\hbar\Omega}{k_B T}) - 2yy' \right) \right]. \quad (21)$$

Comparison of the atomic RDM in the normal phase of Eq.(10) with Eq.(22) shows the two density matrices to be identical provided we make the identifications

$$\begin{aligned} \cosh \beta \Omega &= \left(1 + \frac{2\epsilon_- \epsilon_+}{(\epsilon_- - \epsilon_+)^2 c^2 s^2} \right), \quad (22) \\ m\Omega &= \sqrt{\left(1 + \frac{2\epsilon_- \epsilon_+}{(\epsilon_- - \epsilon_+)^2 c^2 s^2} \right)^2 - 1} \\ &\times \left(\frac{(\epsilon_- - \epsilon_+)^2 c^2 s^2}{2\kappa^2(\epsilon_- c^2 + \epsilon_+ s^2)} \right) \quad (23) \end{aligned}$$

where $\beta = 1/k_B T$. We have two equations linking the four parameters of the atomic RDM ω , ω_0 , λ , κ (where κ is the squeezing parameter we introduced in Eq.(10)) and the three effective parameters of the thermal oscillator β , Ω , m . By setting one energy scale of the original system such that $\omega_0 = 1$, and that of the thermal oscillator such that $m = 1$, $\Omega = \omega$, we can uniquely define the correspondence between the two systems.

The squeezing parameter κ introduced into the RDM in Eq. 10 compensates for the one-mode squeezing that

the atomic ensemble undergoes as a function of λ [16], allowing us to keep the frequency of the thermal oscillator constant. With this relation between the parameters of the two RDMs, the effective temperature becomes the parameter describing the degree of mixing in the RDM. In other words, the interaction of the field with the atomic ensemble is such that, from the point of the atoms alone, it is as if they were at a finite temperature, with the temperature given by Eqs (23). The determination of this temperature is not unique, since there are more free parameters in Eqs (23) than constraints, but the choice made here is physically appealing, with the frequency of the thermal oscillator constant and the temperature varying with λ .

The behavior of the temperature T with λ is shown in Fig. 2, and the divergence at the critical point is immediately obvious. We also plot the squeezing parameter κ , which vanishes at λ_c in accordance with the delocalization of the system here.

The entropy of a harmonic oscillator at finite temperature is a standard result from statistical physics [27] (setting $\hbar = k_B = 1$),

$$S = \left(\frac{\Omega}{2T} \coth\left(\frac{\Omega}{2T}\right) - \ln\left(2 \sinh\left(\frac{\Omega}{2T}\right)\right) \right) / \ln(2). \quad (24)$$

Note that this is independent of κ , and thus the above discussion does not affect the result for S . Solving Eqs (23) for the effective parameters, we obtain the von Neumann entropy of the atom-field system in the normal phase, which is plotted in Fig. 1. The entropy is clearly seen to diverge at λ_c .

Moving into the SR phase, if we calculate the entropy of a single displaced lobe, exactly the same scenario as in the normal phase applies, except with the SR parameters instead of the normal phase ones. Around the critical point, the entropy diverges and then falls to zero for large coupling. As the numerical results show, for large coupling, the finite N results for S do not tend to zero, but rather to a finite value. This can be reconciled with the behavior in the thermodynamic limit by calculating the entropy of the positive-parity two-lobed SR RDM of Eq. (17), rather than the broken-parity single-lobe wave function as above. We recall that this two-lobe RDM is a mixture of the density matrices representing each lobe. A standard result [10] is that for a density matrix $\rho = \lambda_1 \rho_1 + \lambda_2 \rho_2$, $\lambda_{1,2} \geq 0$, the concave nature of the von Neumann entropy allows us to write the following inequality,

$$S(\rho) \geq \lambda_1 S(\rho_1) + \lambda_2 S(\rho_2). \quad (25)$$

The entropy of a mixture of density matrices is also bounded from above by

$$S(\rho) \leq \lambda_1 S(\rho_1) + \lambda_2 S(\rho_2) - \lambda_1 \log \lambda_1 - \lambda_2 \log \lambda_2. \quad (26)$$

The final two terms are known as the mixing entropy [10], and in the case that the ranges of the ρ_1 and ρ_2

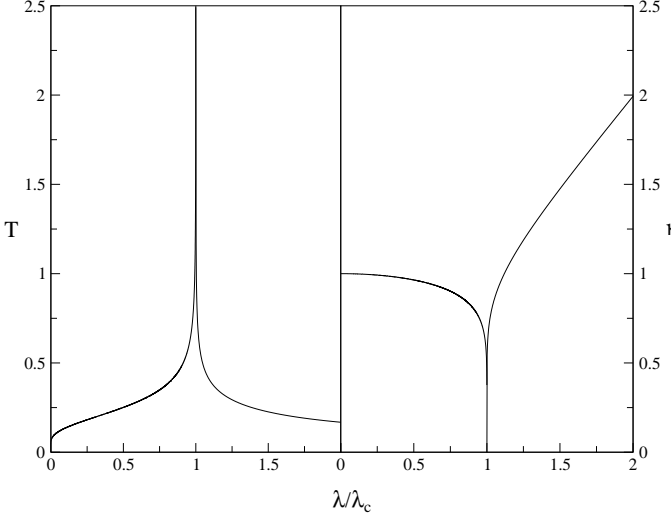


FIG. 2: Effective entanglement temperature T vs. λ/λ_c for $N \rightarrow \infty$, $\omega = \omega_0 = 1$, from Eq. (22) with $\beta = 1/T$. The divergence at the critical point causes the simultaneous divergence of the von Neumann entropy, signalling ‘maximal mixing’. The second graph illustrates the behaviour of the squeezing parameter κ vs λ/λ_c from Eq. (23), which tends to 0 at the critical point.

are pairwise orthogonal, this upper bound becomes an equality.

Returning to our positive-parity SR RDM, the entropy of each of the two lobes is identical $S(\rho_1) = S(\rho_2)$ and they are weighted in an equal superposition $\lambda_1 = \lambda_2 = 1/2$. Furthermore, the two lobes are orthogonal, and thus from Eqs (25,26) we have

$$S(\rho) = S(\rho_1) + 1. \quad (27)$$

This is the form of the SR phase entropy plotted in Fig.(1). We see that by taking into account the parity operator, we obtain the correct high-coupling behavior

From Eq. (24) we see the entropy depends only on the ratio Ω/T . In the limit $\lambda \rightarrow \lambda_c$, we have $\Omega/T \sim \sqrt{\epsilon_-}$. Since as $\lambda \rightarrow \lambda_c$, $\epsilon_- \rightarrow 0$, we see that the effective temperature diverges $T \rightarrow \infty$ and so does the entropy, $S \rightarrow \infty$. In the neighborhood of the critical point, we have

$$\begin{aligned} S_{\lambda \rightarrow \lambda_c} &= [1 - \frac{1}{4} \ln(\frac{64\lambda_c^3\omega^4}{16\lambda_c^4 + \omega^4}) - \frac{1}{4} \ln|\lambda_c - \lambda|]/\ln(2) \\ &= -\frac{1}{4} \log_2 |\lambda_c - \lambda| + \text{const.} \end{aligned} \quad (28)$$

The prefactor to the logarithmic divergence is identical to the exponent characterizing the divergence of the length scale $\nu = 1/4$. Thus we see that, as adjudged by the atom-field entropy, the system is critically entangled.

B. Finite L and N .

We have seen that the entropy diverges logarithmically with $|\lambda - \lambda_c|$. However, in spin-chain systems [6], Latorre *et al* have investigated the behavior of the entropy of L spins cut out from an N spin Hamiltonian, as $N \rightarrow \infty$ at the critical point. Their results suggest $S \sim \log_2(L)$, a result they relate to the scaling of a Conformal Field Theory in the same universality class.

In the thermodynamic limit of our model it is not directly possible to restrict the trace to a finite L of $N \rightarrow \infty$ atoms. However, we can still limit the trace over one of the co-ordinates to a finite Gaussian area L , by artificially introducing a cut-off into the reduced density matrix,

$$\rho_L(x, x') = c_L \int_{-\infty}^{\infty} dy f_L(y) \Psi^*(x, y) \Psi(x', y) \quad (29)$$

with the cut-off function $f_L(x) = e^{-y^2/L^2}$. We perform the trace over the spin system, such that the entropy is equal to the entropy of a Gaussian section of the spin system of area L^2 . Thus, our effective parameters are now given by,

$$\cosh \beta \Omega_L = 1 + 2 \frac{\varepsilon_- \varepsilon_+ + 4(\varepsilon_- c^2 + \varepsilon_+ s^2)/L^2}{(\varepsilon_- - \varepsilon_+)^2 c^2 s^2}. \quad (30)$$

At the critical point, we have $\cosh \frac{\Omega}{T} = 1 + \frac{8}{L^2 \varepsilon_+ c^2}$. Expanding this for $L \rightarrow \infty$, we see that the entropy diverges as a function of L as in the spin-chain systems,

$$S \propto \log_2 [2 \sinh(\frac{2}{L c \sqrt{\varepsilon_+}})] \propto \log_2 L. \quad (31)$$

At $L \rightarrow \infty$ we return to our previous result.

Returning to the numerical data for finite N , we can calculate how the maximum of the entropy scales as a function of N . It is thought that the nature of the scaling of the entropy at the critical point tells us whether that particular quantum phase transition (QPT) can be efficiently classically simulated [6, 8, 28]. We observe,

$$|\lambda_{\max} - \lambda_c| \propto N^{-0.75 \pm 0.1}, \quad S_{\max} \propto (0.14 \pm 0.01) \log_2 N, \quad (32)$$

where λ_{\max} is the position of the entropy maximum. Plots of the numerical data have been discussed in [29] and are therefore not given here.

We mention that while the exponents themselves are difficult to determine accurately with limited numerical data, the maximum of the entropy must scale as a logarithm, and not a power law. This is simply because the dimension of the Hilbert space of Dicke states is $2J + 1 = N + 1$, and thus the maximum possible entropy saturates at $\log_2(N + 1)$. This places the QPT in the Dicke model in the class of systems (alongside one-dimensional spin chains) which are said to be efficient to simulate on a classical computer.

We can also see that the dimensionality of the Hilbert space places restrictions on the value of the scaling

exponent. For our $N + 1$ dimensional Hilbert space, $S_{\max} \propto \log_2(N^a) \leq \log_2(N + 1)$, therefore the exponent $a \leq \log_2(N + 1)/\log_2(N)$. In a general N -spin system the dimension is 2^N , and thus $S_{\max} \propto N^a \leq \log_2(2^N)$, showing that the exponent is $a \leq 1$.

C. Linear Entropy

An alternative measure of entanglement is the linear entropy, given by

$$S_{\text{lin}} = 1 - \text{Tr}(\rho^2), \quad (33)$$

where ρ is the reduced density matrix of one part of our bipartite system. While it is a valid monotonic entanglement measure, it lacks some of the full physical interpretation provided by the von Neumann entropy [11, 30]. Again, we calculate explicit analytical expressions in the thermodynamic limit by employing our co-ordinate space ground state,

$$\begin{aligned} \text{Tr}(\rho^2) &= \int dx dx' \rho(x, x') \rho(x', x) \\ &= \int dx dx' dy dy' \psi(x, y) \psi(x', y) \psi(x, y') \psi(x', y'). \end{aligned} \quad (34)$$

In the normal phase

$$\begin{aligned} S_{\text{lin}} &= 1 - \left(\frac{\epsilon_- \epsilon_+}{(\epsilon_- c^2 + \epsilon_+ s^2)} \right) [(\epsilon_- s^2 + \epsilon_+ c^2)^2 \\ &\quad - \frac{(\epsilon_- s^2 + \epsilon_+ c^2)(\epsilon_- - \epsilon_+)^2 c^2 s^2}{(\epsilon_- c^2 + \epsilon_+ s^2)}]^{-1/2}, \end{aligned} \quad (35)$$

On resonance when $\omega = \omega_0 = 1, c = s = 1/\sqrt{2}$ this simplifies to

$$S_{\text{lin}} = 1 - \frac{2\sqrt{\epsilon_- \epsilon_+}}{(\epsilon_- + \epsilon_+)}, \quad (36)$$

which is zero at zero coupling, and unity at the critical point. In the SR phase we recall the ground state is a superposition of two lobes, and the RDM is a mixture, thus,

$$\text{Tr}(\rho^2) = \frac{1}{4}(\text{Tr}(\rho_1^2) + \text{Tr}(\rho_2^2) + 2\text{Tr}(\rho_1 \rho_2)). \quad (37)$$

As before, the two lobes are pairwise orthogonal, $\text{Tr}(\rho_1^2) = \text{Tr}(\rho_2^2)$, and the cross term is zero. Therefore, we need

$$S_{\text{L}} = 1 - \frac{1}{2}\text{Tr}(\rho_1^2). \quad (38)$$

The explicit expression for this is the same as in the normal phase, but with the above factor $1/2$, and the appropriate SR parameters. In the large coupling limit, $\text{Tr}(\rho_1^2) = 1$, and thus the linear entropy tends to a constant $1/2$, in agreement with the numerics in Fig.1.

There is also a connection between the linear entropy, and the inverse participation ratio [31], a measure of the delocalization of a wave function. The un-normalized inverse participation ratio is defined as,

$$P^{-1} = \int dx dy |\Psi^4(x, y)|, \quad (39)$$

Typically, this is normalized over the volume of the co-ordinate space, however we work with the un-normalized value for convenience. $P^{-1} = 0$ for a state delocalized across the entire co-ordinate space, and $P^{-1} = \text{finite}$ for a localized state, depending on the basis chosen.

We can interpret the participation ratio is a measure of the spread of a wave function over a particular basis, akin to the way the entropy is a measure of the spread of a density matrix over its diagonal basis. In the normal phase, we perform the Gaussian integrals with respect to the spin-boson co-ordinates to obtain

$$P^{-1} = \frac{\sqrt{\epsilon_- \epsilon_+}}{2\pi}. \quad (40)$$

Thus, in this representation, the participation ratio is equal to the Gaussian normalization factor of the ground state, telling us the relative volume in co-ordinate space the state occupies.

In the SR phase, $\Psi_G^{\text{SR}} = \frac{1}{\sqrt{2}}(\psi_1 + \psi_2)$, where $\psi_{1,2}$ represents the two possible displaced lobes. Again, using the fact that there is no overlap between these lobes, we see,

$$P^{-1} = \int dx dy \frac{1}{4}(\psi_1^4 + \psi_2^4) = \int dx dy \frac{1}{2}\psi_1^4(x, y), \quad (41)$$

thus yet again we can use the normal phase result, with the SR phase parameters. This analytical result is plotted in Fig.(1), where the delocalization at the critical point is clearly shown.

IV. PAIRWISE ENTANGLEMENT

To quantify the entanglement between atoms within the ensemble we can no longer use the entropy, since the state of any two atoms will, in general, be mixed. Rather, we employ the concurrence [12, 13], a parameterization of the entanglement of formation commonly applied to two qubits (here, two-level atoms) in a mixed state.

The concurrence is known to vary between 0 for product states, and 1 for maximally entangled states. For a given two-atom mixed density matrix the concurrence is defined as

$$C = \max\{0, \lambda_1 - \lambda_2 - \lambda_3 - \lambda_4\}, \quad (42)$$

where λ_i are the square roots of the eigenvalues in descending order of the matrix

$$\varrho = \rho_{12}(\sigma_{1y} \otimes \sigma_{2y})\rho_{12}^*(\sigma_{1y} \otimes \sigma_{2y}). \quad (43)$$

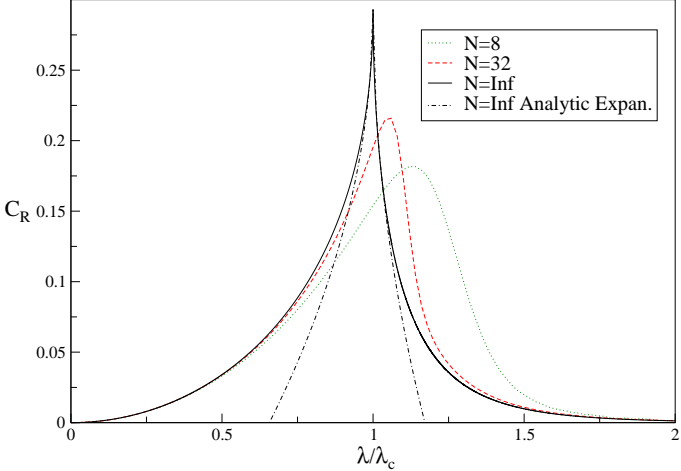


FIG. 3: Re-scaled pairwise concurrence $C_R = NC$ between two spins for systems sizes $N = 8$, $N = 16$, and $N = \infty$. The Hamiltonian is again on scaled resonance $\omega = \omega_0 = 1$. A sharp discontinuity is clearly seen at the critical point in the thermodynamic limit. The non-analyticity of this region is highlighted by a plot of the expansion of the re-scaled concurrence to highest order around the critical point.

where ρ_{12} is the RDM of the two atoms of interest, and σ_{iy} is a Pauli matrix for the i th atom. We make use of the results in Ref. [21] for symmetric states, and express ρ_{12} in terms of the expectation value in the ground state of the collective atomic operators $\langle J_z \rangle$, $\langle J_z^2 \rangle$, and $\langle J_+^2 \rangle$. The matrix elements of ρ_{12} so calculated are given explicitly in Appendix A.

The numerical data shows that the height of the concurrence curve falls as a function of N , therefore we define the re-scaled concurrence as $C_R = NC$. This function is plotted in Fig. 3. It is immediately obvious that there is an N -independent low-coupling region, and scaling behavior around the critical point.

Using the results in Appendix A and first order perturbation theory, we obtain

$$C = \frac{2\sigma^2}{N(1 + \sigma^2)}, \quad \sigma = \lambda/(\omega + \omega_0). \quad (44)$$

for $\lambda \ll \lambda_c$. Thus, we see that at low coupling, the re-scaled concurrence $C_R = NC$ is N -independent. Following the example of [9], we propose that the re-scaled concurrence is the pertinent quantity here, and thus is a feasible measure in its own right.

Exact expressions for the concurrence can be found in the thermodynamic limit using the RDMs derived earlier. The calculations proceeds as follows. We first write the collective spin operators J_i in terms of the Holsten Primakoff representation, and then in the corresponding co-ordinate representation. We then find the expectation values of these operators by tracing over the thermodynamic limit RDMs in the usual fashion $\langle J_i \rangle = \text{Tr}(\rho J_i) = \int dx [J_i(x') \rho(x, x')]_{(x'=x)}$. Details of this calculation are given in appendix B.

A. Normal Phase

In the normal phase we find,

$$C = \frac{2\langle b^\dagger b^\dagger \rangle - 2\langle b^\dagger b \rangle}{(N-1)}, \quad (45)$$

which gives us a rescaled concurrence of,

$$C_R \equiv NC = \left(1 - \frac{m\Omega}{\omega_0} \coth\left(\frac{\Omega}{2T}\right) \right). \quad (46)$$

This expression is plotted alongside the numerical results in Fig. 3. The explicit dependance on λ can be seen by writing

$$\begin{aligned} C_R &= 1 - \frac{\Omega}{\omega_0} \left[\frac{\cosh(\Omega/T) + 1}{\sinh(\Omega/T)} \right] \\ &= 1 - \frac{1}{\omega_0} [(\epsilon_- s^2 + \epsilon_+ c^2)]. \end{aligned} \quad (47)$$

On resonance $\omega = \omega_0$, $\epsilon_- = \omega(1 - 2\lambda/\omega)^{1/2}$, $\epsilon_+ = \omega(1 + 2\lambda/\omega)^{1/2}$, $\lambda_c = \omega/2$ and $s^2 = c^2 = 1/2$. Thus,

$$C_R = 1 - \frac{1}{2} \left((1 - \lambda/\lambda_c)^{1/2} + (1 + \lambda/\lambda_c)^{1/2} \right). \quad (48)$$

from which we see that at the critical point we have $C_R^{\lambda=\lambda_c} = 1 - \frac{1}{\sqrt{2}}$.

We now demonstrate an explicit relation between the concurrence and the spin squeezing. The variance, or uncertainty, in the momentum for the spin system is defined as $(\Delta P_y)^2 = \langle P_y^2 \rangle - \langle P_y \rangle^2$, which in terms of the Holstein-Primakoff operators gives us

$$\begin{aligned} (\Delta P_y) &= \frac{\omega_0}{2} (1 - 2\langle b^\dagger b^\dagger \rangle + 2\langle b^\dagger b \rangle + \langle b^\dagger - b \rangle^2) \\ &= \frac{\omega_0}{2} (1 - 2\langle (b^\dagger)^2 \rangle + 2\langle b^\dagger b \rangle), \end{aligned}$$

since $\langle b^2 \rangle = \langle (b^\dagger)^2 \rangle$, and $\langle b^\dagger - b \rangle^2 = 0$, as any odd terms vanish under the integral with our even-function RDM. Comparison with Eq. (46) yields

$$C_R = 1 - (2/\omega_0)(\Delta P_y)^2. \quad (49)$$

We see that when the spin squeezing is a minimum, the concurrence is a maximum. Similar results have been discussed in [9, 22, 32, 33].

We extract a critical exponent for the non-analyticity in C_R by looking at the derivative of the concurrence (48) near the critical point,

$$\left. \frac{\partial C_R}{\partial \lambda} \right|_{\lambda \rightarrow \lambda_c} \propto |\lambda_c - \lambda|^{-1/2} \quad (50)$$

which exhibits a divergence with the same exponent as the characteristic length scale. The notion of critical entanglement thus applies not only to the atom-field entanglement, but also to the atom-atom entanglement.

B. Superradiant Phase

In the super-radiant phase, we find the re-scaled concurrence is

$$C_R = (1 + \mu)(\langle\langle (d^\dagger)^2 \rangle - \langle d^\dagger d \rangle) + \frac{1}{2}(1 - \mu), \quad (51)$$

where d are displaced Holstein-Primakoff operators of Eq. (11). We find the expectation values of these operators are

$$\langle d^\dagger d \rangle = \left(\frac{\Omega}{4\tilde{\omega}} + \frac{\tilde{\omega}}{4\Omega} \right) \coth \left(\frac{\Omega}{2T} \right) - \frac{1}{2}, \quad (52)$$

$$\langle\langle (d^\dagger)^2 \rangle = - \left(\frac{\Omega}{4\tilde{\omega}} - \frac{\tilde{\omega}}{4\Omega} \right) \coth \left(\frac{\Omega}{2T} \right). \quad (53)$$

Inserting into Eq.(51), and using $\tilde{\omega} = \frac{\omega_0(1+\mu)}{2\mu}$, we find

$$C_R = 1 - \frac{\mu\Omega}{\omega_0} \coth \left(\frac{\Omega}{2T} \right). \quad (54)$$

This function is plotted in Fig. 3. Again, we see precursor behavior, and a non-analyticity at the critical point. As $\lambda \rightarrow \infty$, the re-scaled concurrence tends to zero.

As in the normal phase, we can represent C_R in terms of the coupling and critical coupling alone. However, now the squeezing angle $\gamma^{(2)}$ is always λ dependent,

$$\begin{aligned} C_R &= 1 - \frac{\mu}{\omega_0} \left(\frac{\epsilon_- s^2 + \epsilon_+ c^2}{2} \right) \quad (55) \\ &= 1 - \frac{1}{\sqrt{2}} \frac{\lambda_c^2}{\lambda^2} \left(\left\{ \left(1 + \frac{\lambda^4}{\lambda_c^4} \right) - \left[\left(1 - \frac{\lambda^4}{\lambda_c^4} \right)^2 + 4 \right]^{1/2} \right\}^{1/2} s^2 \right. \\ &\quad \left. + \left\{ \left(1 + \frac{\lambda^4}{\lambda_c^4} \right) + \left[\left(1 - \frac{\lambda^4}{\lambda_c^4} \right)^2 + 4 \right]^{1/2} \right\}^{1/2} c^2 \right) \end{aligned}$$

On resonance, we can summarize the behavior of C_R in the two phases with ($\omega = \omega_0$),

$$\begin{aligned} C_\infty^{x \leq 1} &= 1 - \frac{1}{2} \sum_{\pm} \sqrt{1 \pm x}, \quad x \equiv \lambda/\lambda_c \quad (56) \\ C_\infty^{x \geq 1} &= 1 - \frac{1}{\sqrt{2}x^2} \left[s^2 \sqrt{1 + x^4 - \sqrt{(1 - x^4)^2 + 4}} \right. \\ &\quad \left. + c^2 \sqrt{1 + x^4 + \sqrt{(1 - x^4)^2 + 4}} \right] \end{aligned}$$

A direct series expansion of these expressions to highest order reveals the square-root non-analyticity of the scaled concurrence near the critical point λ_c , $C_R^{\text{NP}} = 1 - 1/\sqrt{2} - (1/2)\sqrt{1-x}$, $C_R^{\text{SR}} = 1 - 1/\sqrt{2} - (1/\sqrt{2})\sqrt{x-1}$. These are plotted alongside the full equation in Fig.(3).

As in the normal phase, there exists a direct relation between the concurrence and the momentum squeezing. Defining

$$(\Delta P_Y)^2 = \frac{\tilde{\omega}}{2} (1 - 2\langle\langle (d^\dagger)^2 \rangle + 2\langle d^\dagger d \rangle) \quad (57)$$

for a single lobe, the concurrence can be written

$$C_R = (1 + \mu) \left(\frac{1}{2} - \frac{1}{\tilde{\omega}} (\Delta P_Y)^2 \right) + \frac{1}{2}(1 - \mu). \quad (58)$$

The critical exponents of the derivatives on this side of the critical point can be extracted from the derivative of (55),

$$\frac{\partial C_R}{\partial \lambda} \Big|_{\lambda \rightarrow \lambda_c} \propto |\lambda_c - \lambda|^{-1/2}. \quad (59)$$

Similar to the analysis in [9], we identify scaling behavior for finite N by calculating the power law behavior of $C_R(\lambda_c) - C_R^M$, the difference between the value of the concurrence at the critical point and the maximum value of the concurrence for a finite N . We observe, as a function of N ,

$$C_R(\lambda_c) - C_R^M = \left(1 - \frac{\sqrt{2}}{2} \right) - C_R^M \sim N^{-0.25 \pm 0.01}. \quad (60)$$

Furthermore, the difference between the point at which the finite size peaks occurs, and the critical point value of λ , is governed by the power law,

$$\lambda_m - \lambda_c \sim N^{-0.68 \pm 0.1}. \quad (61)$$

Plots of the numerical data giving these power laws have been discussed in [29], and are therefore not given here.

V. MULTIPARTITE ENTANGLEMENT AND AVERAGE LOCAL DISORDER

The problem of quantifying the global entanglement in a multipartite system is an open and difficult one, and many different approaches have been proposed (e.g. [34, 35, 36, 37]). A particular example is the measure Q introduced by Meyer and Wallach [14] for pure states of N -qubits. This measure is both easy to calculate and has proved useful in various contexts [38, 39, 40, 41]. As Brennen subsequently showed [41], Q is equal to the average linear entropy of the qubits. As originally intended, this measure applies only to pure states of N qubits, whereas here we have both atoms (qubits) and a bosonic field. Nevertheless, Brennen's result implies that we may obtain a useful measure of the entanglement in the atomic ensemble by considering the average linear entropy of the RDM of each atom after tracing out both the rest of the atoms *and* the field mode. Thus, as measure of the global entanglement in the atom system we consider the average linear entropy, defined by

$$Q \equiv 2 \left(1 - \frac{1}{N} \sum_{k=0}^{N-1} \text{Tr}(\rho_k^2) \right), \quad (62)$$

where ρ_k is the RDM of the k th atom with both other atomic and bosonic degrees of freedom traced out. Q is a measure of the average local disorder in the system.

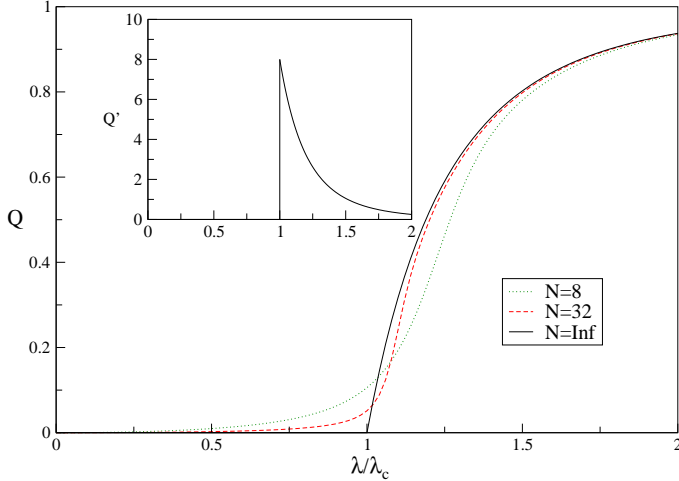


FIG. 4: The Meyer-Wallach multipartite measure Q from Eq. (63) applied to our atomic mode for system sizes $N = 8$, $N = 16$, and $N = \infty$. As discussed in the text, this is equivalent to the linear entropy of a single atom in the atomic mode, or ‘the average single atom disorder’. In the thermodynamic limit normal phase $Q = 0$. This is not in conflict with the finite re-scaled concurrence result, which is also a (minimized) measure of single atom disorder or mixing, as we re-scale the concurrence by N . (Inset: The derivative of Q in the thermodynamic limit $\frac{\partial Q}{\partial \lambda}$, illustrating the discontinuity at the critical point).

We now calculate Q for the ground state of our model. Since the Dicke states are symmetric with respect to interchange of atoms, the average over k is identical to the value for one atom. Furthermore, we can express Q in terms of the collective operators

$$\begin{aligned} Q &= 1 - 4\langle J_z \rangle^2/N^2 - 4\langle J_- \rangle \langle J_+ \rangle / N^2 & (63) \\ &= 1 - 4\langle J_z \rangle^2/N^2 \end{aligned}$$

since the expectation value of the raising and lowering operators is always zero. In the normal phase $\langle J_z \rangle^2 = \langle b^\dagger b \rangle^2 - N\langle b^\dagger b \rangle + N^2/4$, and thus in the thermodynamic limit we have $Q_{N \rightarrow \infty}^{\lambda < \lambda_c} = 0$. In the super-radiant phase, $\langle J_z \rangle^2 = \langle d^\dagger d \rangle^2 - N\mu\langle d^\dagger d \rangle + N^2\mu^2/4$, and thus $Q_{N \rightarrow \infty}^{\lambda > \lambda_c} = (1 - \mu^2)$. These results are plotted in Fig.(4), along with numerical results for finite N .

There is clearly a discontinuity between the two phases, as can be seen in Fig.(4). This follows directly from the discontinuity of the atomic inversion at the critical point [16]. As a final point, the derivative of Q in the SR phase TD limit is $\frac{\partial Q}{\partial \lambda} = 4\lambda_c^4/\lambda^5$, which we plot as an inset in the figure.

VI. DISCUSSION AND CONCLUSIONS

In summary, we calculated the entanglement properties for three partitions of the Dicke Model; between the atomic ensemble and the field mode, between pairs of

atoms, and a multipartite partition which we found is equivalent to a partition between a single atom and the rest of the system.

Table I presents the most important results for the three entanglement measures we have calculated, and where appropriate their derivatives. In particular, we point out the importance of the divergences at the critical point, and the scaling exponents.

| $f(\lambda)$ | $f(\lambda \rightarrow \lambda_c)$ | N Scaling |
|---|---|------------------------------|
| ϵ_- | $ \lambda_c - \lambda ^{1/2}$ | - |
| l_- | $ \lambda_c - \lambda ^{-1/4}$ | - |
| S | $-\frac{1}{4} \log_2 \lambda - \lambda_c $ | $\log_2 N^{(0.14 \pm 0.01)}$ |
| C_R | $1 - \frac{\sqrt{2}}{2}$ | $N^{-0.25 \pm 0.01}$ |
| $\frac{\partial C_R}{\partial \lambda}$ | $ \lambda_c - \lambda ^{-1/2}$ | - |
| Q | 0 | - |

TABLE I: Entropy S , Eq. (24), concurrence C_R , Eq. (48) and Eq. (55), and Meyer-Wallach entanglement Eq. (63), in the Dicke model near the critical point $\lambda \rightarrow \lambda_c$

For the atom-boson partition, we calculated the entropy exactly in the thermodynamic limit and numerically for finite N . The entropy has a divergence around $\lambda = \lambda_c$, which follows the power law divergence of the correlation length $l_- \propto |\lambda - \lambda_c|^{-1/4}$. The scaling of the entropy with the system size N and with a finite Gaussian block of atoms defined by an area L is logarithmic, thus relating the phase transition of the Dicke model to a class containing one-dimensional spin-chain systems and Conformal Field Theories [6].

There is also a correspondence between the divergence of the spin-boson entanglement (entropy) and the delocalization of the wave function. This is highlighted by our results for the behavior of the participation ratio, which shows that the ground state of the Dicke model undergoes a massive delocalization at the critical point. Since delocalization is a common property of wave functions in a quantum chaotic system, our results help strengthen the understanding of the relationship between entanglement and the underlying integrable to chaotic transition present in the Dicke Hamiltonian [16]. However, most *generic* features of this relationship are still unknown. The future of this field lies in closer examination of the underlying semi-classical behavior in quantum systems, such as supercritical pitchfork bifurcations [17] in coordinate space, or phase space.

For the entanglement between pairs of atoms, we have calculated the re-scaled pairwise concurrence. This re-scaled concurrence reaches a maximum at the critical point, with a divergence in its derivative. It also exhibits finite size scaling behavior, similar to that seen in a related simplex model [9]. Similarly, we have calculated an extension of the Meyer-Wallach multipartite entanglement which has a clear discontinuity at the critical point in the thermodynamic limit.

We hope that future research may arise from investigating quantum phase transitions in other spin-boson

models [16, 17]. In particular, while the Dicke model has a natural feature that allows infinite system sizes to be investigated, there is no reason other spin-boson models with non-commuting energy and interaction terms which do not have this integrable limit should not exhibit similar critical entanglement, with chaotic transitions and level statistics.

Acknowledgments

This work was supported by projects EPSRC GR44690/01, DFG Br1528/4-1, the WE Heraeus foundation, the Dutch Science Foundation NWO/FOM, and the UK Quantum Circuits Network.

APPENDIX A: PAIRWISE DENSITY MATRIX ELEMENTS

The RDM of two spins from a symmetric Dicke state is,

$$\rho_{12} = \begin{bmatrix} \mu_+ & x_+ & x_+ & u \\ x_+ & w & y & x_- \\ x_+ & y & w & x_- \\ u & x_- & x_- & \mu_- \end{bmatrix} \quad (\text{A1})$$

where the matrix elements, as derived in [21], are given by

$$\mu_{\pm} = \frac{N^2 - 2N + 4\langle J_z^2 \rangle \pm 4\langle J_z \rangle(N-1)}{4N(N-1)}, \quad (\text{A2})$$

$$x_{\pm} = \frac{(N-1)\langle J_+ \rangle \pm \langle [J_+, J_z]_+ \rangle}{2N(N-1)}, \quad (\text{A3})$$

$$w = \frac{N^2 - 4\langle J_z^2 \rangle}{4N(N-1)}, \quad y = \frac{2\langle J_x^2 + J_y^2 \rangle - N}{2N(N-1)}, \quad (\text{A4})$$

$$u = \frac{\langle J_+^2 \rangle}{N(N-1)}. \quad (\text{A5})$$

In numerical calculations, one can use the following expressions in terms of the reduced spin density matrix ρ_{mn} ,

$$\langle J_z \rangle = \sum_{m=-j}^{+j} \rho_{mm} m, \quad \langle J_z^2 \rangle = \sum_{m=-j}^{+j} \rho_{mm} m^2, \quad (\text{A6})$$

$$\langle J_+ \rangle = \sum_{m=-j}^{+j} \rho_{mm+1} (j(j+1) - m(m+1)), \quad (\text{A7})$$

$$\begin{aligned} \langle J_+^2 \rangle &= \sum_{m=-j}^{+j} \rho_{mm+2} (j(j+1) - m(m+1)) \\ &\times (j(j+1) - (m+1)(m+2)), \end{aligned} \quad (\text{A8})$$

$$\langle [J_+, J_z]_+ \rangle = \sum_{m=-j}^{+j} \rho_{mm+1} (j(j+1) - m(m+1)) (2m+1), \quad (\text{A9})$$

$$\langle J_x^2 + J_y^2 \rangle = \langle J^2 - J_z^2 \rangle = \sum_{m=-j}^{+j} \rho_{mm} (j(j+1) - m^2). \quad (\text{A10})$$

The non-zero expectation values of the collective operators for the perturbed density matrix are,

$$\langle J_z \rangle = \frac{-j}{1+\sigma^2} + \frac{\sigma^2}{1+\sigma^2} (-j+1), \quad (\text{A11})$$

$$\langle J_z^2 \rangle = \frac{j^2}{1+\sigma^2} + \frac{\sigma^2}{1+\sigma^2} (-j+1)^2, \quad (\text{A12})$$

$$\langle J_+ \rangle = 0, \quad \langle J_+^2 \rangle = 0, \quad \langle [J_+, J_z]_+ \rangle = 0, \quad (\text{A13})$$

$$\langle J_x^2 + J_y^2 \rangle = \frac{j(j+1) - j^2}{1+\sigma^2} + \frac{\sigma^2}{1+\sigma^2} (j(j+1) - (-j+1)^2). \quad (\text{A14})$$

APPENDIX B: ELEMENTS IN THE THERMODYNAMIC LIMIT

In the thermodynamic limit, the parity symmetry is still conserved below the phase transition, and above it when we consider both lobes, thus $\langle S_+ \rangle = 0$. Therefore, the general form of the reduced density matrix is

$$\rho_{12} = \begin{bmatrix} \mu_+ & 0 & 0 & u \\ 0 & w & w & 0 \\ 0 & w & w & 0 \\ u & 0 & 0 & \mu_- \end{bmatrix}. \quad (\text{B1})$$

The four eigenvalues are $\lambda_1 = (\sqrt{\mu_+\mu_-} - u)^2$, $\lambda_2 = (\sqrt{\mu_+\mu_-} + u)^2$, $\lambda_3 = 4y^2$, $\lambda_4 = 0$. Therefore the concurrence depends on the relative magnitude of $2y$ and $|(\sqrt{\mu_+\mu_-} + u)|$. Thus,

$$\text{if } 2y < |\sqrt{\mu_-\mu_+} + u|, \quad (\text{B2})$$

$$\begin{aligned} C &= \max\{0, |\sqrt{\mu_-\mu_+} + u| - |\sqrt{\mu_-\mu_+} - u| - 2y\} \\ &= 2|u| - 2y. \end{aligned}$$

$$\text{If } 2y \geq u,$$

$$\begin{aligned} C &= \max\{0, 2y - |\sqrt{\mu_-\mu_+} + u| - |\sqrt{\mu_-\mu_+} - u|\} \\ &= 2y - 2\sqrt{\mu_-\mu_+}. \end{aligned}$$

This form is identical to the Kitagawa-Ueda state example from [21], where the matrix elements depend on three expectation values $\langle J_z \rangle$, $\langle J_z^2 \rangle$ and $\langle J_+^2 \rangle$.

1. Normal Phase

Substituting the normal phase Holstein-Primakoff transformations into the expectation values,

$$\langle J_z \rangle = \langle (b^\dagger b - j) \rangle \approx -j = N/2, \quad (\text{B3})$$

$$\begin{aligned} \langle J_z^2 \rangle &= \langle (b^\dagger b - j)^2 \rangle \\ &\approx -2j\langle b^\dagger b \rangle + j^2 = -N\langle b^\dagger b \rangle + N^2/4, \end{aligned} \quad (\text{B4})$$

$$\begin{aligned} \langle J_+^2 \rangle &= \langle (b^\dagger \sqrt{2j - b^\dagger b})^2 \rangle \\ &\approx \langle b^\dagger b^\dagger \rangle (2j - \sqrt{2j}) = \langle b^\dagger b^\dagger \rangle (N - \sqrt{N}), \end{aligned} \quad (\text{B5})$$

in the limit of $N \rightarrow \infty$. We work only to order $O(N)$ or higher. In this lowest order, the element μ_+ is zero, but in full we have

$$\mu_+ = \frac{4(\langle (b^\dagger b)^2 \rangle - \langle b^\dagger b \rangle)}{4N(N-1)}. \quad (\text{B6})$$

Similarly, μ_- is

$$\mu_- = \frac{4N^2 - 4N - 8N\langle b^\dagger b \rangle + 4\langle b^\dagger b \rangle + 4(\langle b^\dagger b \rangle^2)}{4N(N-1)}. \quad (\text{B7})$$

Thus, to $O(N)$, $\sqrt{\mu_+ - \mu_-}$ is non-zero when $N \rightarrow \infty$,

$$\sqrt{\mu_+ - \mu_-} = \frac{4N(\langle (b^\dagger b)^2 \rangle - \langle b^\dagger b \rangle)^{1/2}}{4N(N-1)}. \quad (\text{B8})$$

The other two elements are

$$y = \frac{N^2 - 4\langle S_z^2 \rangle}{4N(N-1)} \approx \frac{4N\langle b^\dagger b \rangle}{4N(N-1)}, \quad (\text{B9})$$

and

$$u = \frac{4\langle S_+^2 \rangle}{N(N-1)} \approx \frac{4N\langle b^\dagger b^\dagger \rangle}{4N(N-1)}. \quad (\text{B10})$$

For the $2y < |\sqrt{\mu_+ - \mu_-} + u|$ case, that the concurrence reduces to

$$C = \frac{2\langle b^\dagger b^\dagger \rangle - 2\langle b^\dagger b \rangle}{(N-1)}, \quad (\text{B11})$$

and for the $2y \geq |\sqrt{\mu_+ - \mu_-} + u|$ case,

$$C = \frac{2\langle b^\dagger b \rangle - 2(\langle (b^\dagger b)^2 \rangle - \langle b^\dagger b \rangle)^{1/2}}{(N-1)}. \quad (\text{B12})$$

In both cases $C_R = CN$ has a finite value.

To obtain the expectation values of the b operators, one must express them in their co-ordinate representation, and find the expectation value from the integral over the reduced density matrix. We work with the reduced density matrix in effective temperature form. Recalling that

$$b^\dagger = \sqrt{\frac{\omega_0}{2}}(y - \frac{iP_y}{\omega_0}), \quad (\text{B13})$$

$$b^\dagger b = \frac{\omega_0 y^2}{2} - \frac{1}{2\omega_0} \partial_y^2 - \frac{1}{2}, \quad (\text{B14})$$

and,

$$b^\dagger b^\dagger = \frac{\omega_0 y^2}{2} + \frac{1}{2\omega_0} \partial_y^2 - \frac{y\partial_y}{2} - \frac{\partial_y y}{2}, \quad (\text{B15})$$

the following results are easily shown,

$$\langle \frac{-\partial_y^2}{2\omega_0} \rangle = \frac{\Omega}{4\omega_0} \coth(\frac{\Omega}{2T}), \quad (\text{B16})$$

$$\langle \frac{\omega_0 y^2}{2} \rangle = \frac{\omega_0}{4\Omega} \coth(\frac{\Omega}{2T}), \quad (\text{B17})$$

$$\langle -\frac{y\partial_y}{2} - \frac{\partial_y y}{2} \rangle = \langle -\frac{2y\partial_y}{2} - \frac{1}{\omega_0} \rangle = 0. \quad (\text{B18})$$

Thus,

$$\langle b^\dagger b \rangle = \left(\frac{m\Omega}{4\omega_0} + \frac{\omega_0}{4m\Omega} \right) \coth(\frac{\Omega}{2T}) - \frac{1}{2} \quad (\text{B19})$$

and,

$$\langle b^\dagger b^\dagger \rangle = -\left(\frac{m\Omega}{4\omega_0} - \frac{\omega_0}{4m\Omega} \right) \coth(\frac{\Omega}{2T}) \quad (\text{B20})$$

Looking at the inequalities numerically, $2y < |\sqrt{\mu_- - \mu_+} + u|$ always holds.

2. Super-Radiant Phase

In the super-radiant phase, when calculating the expectation value of one of the collective spin operators J_i , we again need to use the two-lobed ground state. We can write

$$\langle J_i \rangle = \text{tr}(\rho_{\text{spin}} J_i) = \frac{1}{2} (\text{tr}(\rho_1 J_i) + \text{tr}(\rho_2 J_i)). \quad (\text{B21})$$

$\rho_{1,2}$ are the states displaced by $\pm\sqrt{\beta}$ respectively. However, it is more convenient to displace the operators J_i by writing them in terms of b, b^\dagger and then displacing these as $b = d \pm \sqrt{\beta}$. We then find the expectation value using the original $\rho = \rho_1 = \rho_2$, the undisplaced density matrix

equivalent to the density matrix of a thermal harmonic oscillator.

When combining the contributions from both lobes in Eq.(B21), odd powers of $\sqrt{\beta}$ will cancel. Also, again we use the simplification that the lobe wave functions are even functions, and only even combinations of creation and annihilation operators will produce non-zero results. Hence, as in the normal phase, only the elements μ_{\pm}, ω and u are non-zero.

Working with the $-\sqrt{\beta}$ displacements, and then making the above simplifications (including keeping only terms $O(N)$ or greater), we have

$$\begin{aligned} \langle J_z \rangle &= \langle b^\dagger b - j \rangle \\ &= \langle d^\dagger d - \sqrt{\beta}(d + d^\dagger) + \beta - j \rangle = \langle d^\dagger d \rangle - \frac{N}{2}\mu, \end{aligned} \quad (\text{B22})$$

$$\begin{aligned} \langle J_z^2 \rangle &= \langle (d^\dagger d)^2 \rangle + N(1 - 2\mu)\langle d^\dagger d \rangle \\ &+ N(1 - \mu)\langle (d^\dagger)^2 \rangle + \frac{N}{2}(1 - \mu) + N^2\mu^2/4, \end{aligned} \quad (\text{B23})$$

where again we have used $\langle (d^\dagger)^2 \rangle = \langle d^2 \rangle$, and $\langle d + d^\dagger \rangle = 0$. Similarly,

$$\begin{aligned} \langle J_+^2 \rangle &= \frac{N}{2}(3\mu - 1)\langle (d^\dagger)^2 \rangle - \frac{3N}{2}(1 - \mu)\langle d^\dagger d \rangle \\ &- \frac{N}{4}(1 - \mu) + \frac{N^2}{4}(1 - \mu^2). \end{aligned} \quad (\text{B24})$$

Thus, the important matrix elements become,

$$\begin{aligned} \omega &= \frac{1}{4}(1 - \mu^2) \\ &- \frac{1}{N} \left((1 - 2\mu)\langle d^\dagger d \rangle + (1 - \mu)\langle (d^\dagger)^2 \rangle + \frac{1}{2}(1 - \mu) \right), \end{aligned} \quad (\text{B25})$$

$$\begin{aligned} u &= \frac{1}{4}(1 - \mu^2) \\ &+ \frac{1}{2N} \left(-3(1 - \mu)\langle d^\dagger d \rangle + (3\mu - 1)\langle (d^\dagger)^2 \rangle - \frac{1}{2}(1 - \mu) \right), \end{aligned} \quad (\text{B26})$$

$$\begin{aligned} \mu_{\pm} &= \frac{1}{4}(1 \pm \mu)^2 \\ &+ \frac{1}{N} \left((1 \pm 1 - 2\mu)\langle d^\dagger d \rangle + (1 - \mu)\langle (d^\dagger)^2 \rangle - \frac{1 \mp 1}{2}\mu \right). \end{aligned} \quad (\text{B27})$$

Again, one is faced with an inequality depending on the relative values of combinations of the matrix elements of the two-atom reduced density matrix. However, looking at these numerically we observe that again the concurrence is given by $C = 2\max(0, u - \omega)$. Inserting u and ω gives the results we show in the main text.

[1] S. Sachdev *Quantum Phase Transitions*, (Cambridge University Press, 1999).
[2] M. C. Gutzwiller, *Chaos in Classical and Quantum Mechanics*, (Springer, 1990).
[3] T. J. Osborne and M. A. Nielsen, Phys. Rev. A **66**, 032110 (2002).
[4] A. Osterloh, L. Amico, G. Falci, R. Fazio, Nature **416**, 608 (2002).
[5] G. Vidal, J. I. Latorre, E. Rico, and A. Kitaev, Phys. Rev. Lett. **90**, 227902.
[6] J. I. Latorre, E. Rico, and G. Vidal, Quant. Inf. and Comp. **4**, 1 (2004).
[7] M. Srednicki, Phys. Rev. Lett. **71**, 666 (1993).
[8] R. Orús and J.I. Latorre, quant-ph/0308042.
[9] J. Vidal, G. Palacios, and R. Mosseri, Phys. Rev. A **69**, 022107 (2004).
[10] A. Wehrl, Rev. Mod. Phys. **50**, 221 (1978).
[11] B. Schumacher, Phys. Rev. A **51**, 2738 (1993).
[12] C. H. Bennett, D. P. DiVincenzo, J. A. Smolin, and W. K. Wootters, Phys. Rev. A **54**, 3824 (1996).
[13] W. K. Wootters, Phys. Rev. Lett. **80**, 2245 (1997).
[14] D. A. Meyer and N. R. Wallach, quant-ph/0108104.
[15] C. Emary and T. Brandes, Phys. Rev. Lett. **90**, 044101 (2003).
[16] C. Emary and T. Brandes, Phys. Rev. E **67**, 066203 (2003).
[17] A. P. Hines, G.J. Milburn, and R. H. McKenzie, quant-ph/0308165.
[18] S. Schneider, and G. J. Milburn, Phys. Rev. A **65**, 042107 (2002).
[19] H. Fujisaki, T. Miyadera, and A. Tanaka, Phys. Rev. E **67**, 066201 (2003).
[20] T. Vorrath and T. Brandes, Phys. Rev. B **68**, 035309 (2003).
[21] X. Wang and K. Mølmer, Eur. Phys. J. D **18**, 385 (2002).
[22] X. Wang, M. Feng, and B. C. Sanders, Phys. Rev. A **67**, 022302 (2003).
[23] M. B. Plenio and S. F. Huelga, Phys. Rev. Lett. **88**, 197901 (2002).
[24] T. Brandes and N. Lambert, Phys. Rev. B **67**, 125323 (2003).
[25] C. Emary, PhD Thesis, UMIST, Manchester (UK), unpublished (2001).
[26] M. Frasca, quant-ph/0312203.
[27] R. P. Feynman, *Statistical Mechanics* (The Perseus Books Group, 1998).
[28] G. Vidal, Phys. Rev. Lett. **91**, 147902 (2003).
[29] N. Lambert, C. Emary and T. Brandes, Phys. Rev. Lett. **92**, 073602 (2004).
[30] C. H. Bennett, H. J. Bernstein, S. Popescu, B. Schumacher, Phys. Rev. A **53**, 2046 (1996).
[31] J. T. Edwards and D. J. Thouless, J. Phys. C: Solid State Phys **5**, 8 (1972).
[32] M. Kitagawa and M. Ueda, Phys. Rev. A **47**, 5138, (2003).
[33] D. Ulam-Orgikh and M. Kitagawa, Phys. Rev. A **64**, 052106 (2001).

- [34] N. Linden, S. Popescu, and A. Sudbery, Phys. Rev. Lett. **83**, 243 (1999).
- [35] H. A. Carteret, N. Linden, S. Popescu, and A. Sudbery, Found. Phys. **29**, 527 (1999).
- [36] A. Miyake, Phys. Rev. A **67**, 012108 (2003).
- [37] F. Verstraete, J. Dehaene, and B. De Moor, Phys. Rev. A **68**, 012103 (2003).
- [38] A. J. Scott, quant-ph/0310137.
- [39] R. Somma, G. Ortiz, H. Barnum, E. Knill, and L. Viola, quant-ph/0403035
- [40] A. J. Scott and C. M. Caves, J. Phys. A **36**, 9553 (2003).
- [41] G. K. Brennen, Quantum Information and Computation **3**, 619 (2003).